IEEE Access
Multidisciplinary | Rapid Review | Open Access Journal

Received February 10, 2021, accepted March 22, 2021, date of publication March 24, 2021, date of current version April 7, 2021.

Digital Object Identifier 10.1109/ACCESS.2021.3068949

Robust Control Framework for Lateral Dynamics of Autonomous Vehicle Using Barrier Lyapunov Function

RAMEEZ KHAN, FAHAD MUMTAZ MALIK, NAVEED MAZHAR, ABID RAZA, RAJA AMER AZIM, AND HAMEED ULLAH

College of Electrical Engineering and Mechanical Engineering, National University of Sciences and Technology (NUST), Islamabad 44000, Pakistan

Corresponding author: Rameez Khan (rameez.khan@ceme.nust.edu.pk)

This work was supported by the National University of Sciences and Technology, Pakistan.

ABSTRACT This article presents the robust lateral control of an autonomous vehicle in the presence of unknown lateral tire forces, road curvature angle, and parametric uncertainties. The sliding mode control (SMC) with barrier Lyapunov function is implemented to guarantee the system robustness while maintaining the outputs of the system in realistic bounds. Following the model reduction approach, the slow and fast dynamics of the system are separately controlled using the proposed control technique. The efficacy of the proposed control technique is examined by comparing the simulation results with conventional sliding mode control in two-time scales.

INDEX TERMS Autonomous vehicle, barrier function, lateral dynamics, nonlinear model reduction, output constraints, single-input multi-output control, two-time scales.

I. INTRODUCTION

The development of autonomous vehicles has remained an interesting field of research for academia, the car manufacturing industry, and other companies for the last three decades [1]. The autonomy of the vehicles is beneficial to society in several ways including passenger comfort, reduction in road accidents, and optimal fuel consumption. With the advancements in the development of autonomous vehicles, there are several challenges associated with it, including vehicle and passenger safety, fuel efficiency, and efficient maneuvering in different environments on different terrains [2]. The efficient maneuvering of the autonomous vehicle is of paramount importance, therefore significant research is being carried out to address the problems including vehicle stabilization in a cluttered environment, path tracking in presence of uncertainties and disturbances, localization, navigation, obstacle avoidance, and steering control while catering road bank angle and slippage etc. [3]–[7].

Path tracking control is a key concern for the autonomous vehicle during motion. The path tracking control enables the autonomous vehicle to track the desired trajectory by adjusting the lateral and longitudinal motion of the vehicle. In the car-like autonomous vehicle, the longitudinal dynamics become dominant when moving along the straight path while moving on the curved path, the lateral dynamics become more significant [8]. Autonomous vehicles require longitudinal and lateral control to achieve the desired path tracking [9]. The longitudinal control is to cater to the challenges of desired acceleration and operations of accelerating and braking of the vehicle [10]. On the other hand, lateral control deals with the challenges of safety, lane-keeping, lane changing, and achieving the desired lateral position [11], [12]. This article focuses on the robust control design for the lateral dynamics of the autonomous vehicle moving on the curve path.

Lateral control for the autonomous vehicle has remained a challenging task for researchers due to the complicated lateral dynamics. Several studies are found in the literature to design the different control topologies for the autonomous vehicle lateral dynamics including LQR [13], PID [14], feedback linearization [15] backstepping [16], [17], gain scheduling [18], sliding mode control (SMC) [19], [20], and fuzzy logic [21], [22]. The steering control for the autonomous vehicle using SMC and the backstepping controller is proposed in [19]. In [23] the sliding mode variable structure is adopted to control the lateral dynamics of the vehicle. The SMC in conjunction with gain scheduling and disturbance observer is presented in [24] for the vehicle path tracking.

The associate editor coordinating the review of this manuscript and approving it for publication was Luigi Biagiotti.

Generally, the autonomous car-like vehicles are modeled with the 3 degrees of freedom (DOF) bicycle model. Moreover, with the assumption that the longitudinal dynamics are smooth and entirely controlled by the longitudinal controller, the system model is reduced to 2-DOF i.e. yaw and lateral position. This modifies the autonomous vehicle model into a single-input multi-output (SIMO) system. The SIMO model of the autonomous vehicle has two outputs, yaw angle, and lateral position. Intuitively, the lateral position is a slow state while the yaw angle is a fast state. Hence, the autonomous vehicle lateral dynamics can be reduced to slow and fast dynamics. These fast and slow systems are usually controlled by devising a two-time scale-based controller approach. Mostly, SIMO systems are controlled using energy-based controllers [25], intelligent controllers [26], [27], hierarchical controllers [28]–[31], and multi-time scale based controllers [32], [33]. This article uses the reduced-order model based on the two-timescale approach to design the control for lateral dynamics of the autonomous vehicle.

Another important prospect of the autonomous vehicle is its safety and stability when prone to an uncertain environment. Due to saturation and nonlinear tire-terrain dynamics, the vehicle can maneuver in unsafe operating range. One of the solutions to this problem lies in restricting the system states in certain bound. These constraints are usually fulfilled by using a control barrier function [34], [35]. In [34], the barrier function in conjunction with SMC is used to constraint the output of the quadrotor with modeling uncertainties and disturbances. In [35], a hierarchical controller-based approach is used for lateral control for the vehicle. The authors have used the barrier function to constraint the yaw rate and sideslip angle for the multi-input multi-output (MIMO) model and linear tire dynamics. Although several other studies have employed barrier function [36], [37], no significant research exists regarding barrier function with SMC for the autonomous vehicles' lateral dynamics in the presence of nonlinear tire-forces, curvature angle, and parametric uncertainties.

In this article, the control of the lateral dynamics of the car-like autonomous vehicle is considered, while moving on the curved path. The vehicle is modeled using the 2-DOF bicycle model by incorporating the impact of the lateral tire forces, parametric uncertainties, and road curvature. This modifies the autonomous vehicle model into a SIMO system with yaw and lateral position as its outputs and steering angle as the input. The control design becomes challenging in the presence of nonlinear tire forces and road curvature in the vehicle model. Following the approach used in [38]–[40], the system model is reduced into slow and fast subsystem with lateral position having slow dynamics while the yaw having fast dynamics. This allows designing the two separate controllers by inducing an auxiliary control input in slow dynamics which reduces the complexity of the control design. To keep the states in lateral position and yaw angle in realistic bounds in presence of the aforementioned disturbances, the approach of [34] is modified for both subsystems. Furthermore, the finite-time convergence advantage of the control approach helps in choosing the controller gains systematically. Finally, the comparison of the proposed control technique with conventional SMC is carried out using numerical simulation, which proves the efficacy of the proposed technique.

The overall contribution of this article is stated as follows: i) The proposed control guarantees the tracking of lateral dynamics in presence of modeling uncertainties, lateral tire forces due to slip and road banking. ii) The yaw angle and lateral position are bounded by certain realistic upper and lower bounds. iii) different from existing literature, the proposed methodology provides a novel control scheme for SIMO perturbed systems under state constraints.

The remaining article is structured in the following way: the necessary lemmas and assumptions for control design are defined in Section II. The lateral dynamics of the autonomous vehicle are modeled in Section III. In Section IV, the conventional SMC and SMC with barrier function is developed and implemented for the reduced-order system model for controlling the lateral dynamics of the autonomous vehicle. In Section V MATLAB/Simulink based simulation result are presented and discussed. Section VI concludes the paper.

II. PRELIMINARIES

The nonlinear second-order system is given by

$$\dot{x}_1 = x_2 \tag{1}$$

$$\dot{x}_2 = f(x) + g(x)\,u + D(x,t) \tag{2}$$

$$y = x_1 \tag{3}$$

where the systems' states are $x_1, x_2 \in \mathbb{R}$, input $u \in \mathbb{R}$, output $y \in \mathbb{R}$ and f and g are the smooth functions and uncertainties are given by $D(x,t)$. The initial conditions are $x(0) = x_0 = [x_{10}\, x_{20}]$. The output $y(t)$ should track the desired output $y_d(t)$ while remaining in a certain bound i.e. $|y(t)| \leq \hbar_c \forall t \geq 0$, where $\hbar_c$ is a positive constant.

Definition 1 [34]: For a system $\dot{x} = f(x)$, a barrier Lyapunov function $V(x)$ is a scalar function, which is continuously differentiable such that $x \in \mathcal{D}$ and $V(x) \to \infty$ as x approaches to $\partial\mathcal{D}$, and satisfies $V(x) \leq a, \forall t \geq 0$ for some positive constant a.

Assumption 1: For any $\hbar_c > 0$, there exist positive constants $\underline{Y_0}, \overline{Y}_0, A_0, Y_1, Y_2, \ldots, Y_n$ satisfying $\max\left\{\underline{Y_0}; \overline{Y}_0\right\} \leq A_0 < \hbar_c$ such that the desired trajectory $y_d(t)$ and its time derivatives satisfy $\underline{Y_0} \leq y_d(t) < \overline{Y}_0, |\dot{y}_d(t)| \leq Y_1, \ldots, \left|y_d^{(n)}(t)\right| \leq Y_n$ for all $t \geq 0$.

Lemma 1 [41]: For the system (1) with any $\hbar_b > 0$, consider $\mathcal{E}1 := \{\xi_1 \in \mathbb{R} : -\hbar_b < \xi_1 < \hbar_b\} \subset \mathbb{R}$. Let V_1 and V_2 are positive definite and continuously differentiable functions in their respective domain as $V_1(x_1) \to \infty$ as $x_1 \to \hbar_b$ or $x_1 \to -\hbar_b$ and

$$\underline{\beta}(|x_2|) \leq V_2(x_2) \leq \overline{\beta}(|x_2|) \tag{4}$$

Here $\overline{\beta}$s and $\underline{\beta}$ are class $\mathcal{K}_\infty$ functions. Let V_1 and V_2 are functions that imply $V(x) = V_1(x_1) + V_2(x_2)$ and x_1 belong

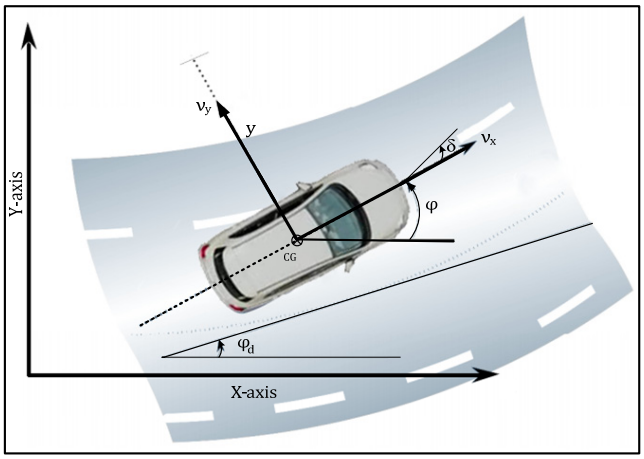

FIGURE 1. Autonomous vehicle on the curved path.

to the set $x_1 \in (-\hbar_b, \hbar_b)$. If

$$\dot{V} = \frac{\partial V}{\partial x}\dot{x} \leq 0 \tag{5}$$

then $x_1(t)$ remains in the open set $x_1 \in (-\hbar_b, \hbar_b)\ \forall t \geq 0$.

Lemma 2 [42], [43]: For any positive constant a, b, the following inequality holds $\forall x$ such that $|x| < a$:

$$(a+b)^{\wp} \leq a^{\wp} + b^{\wp} \tag{6}$$

where $0 < \wp \leq 1$, and

$$\ln\left(\frac{a^2}{a^2 - x^2}\right) \leq \frac{x^2}{a^2 - x^2} \tag{7}$$

$\forall x$ such that $|x| < a$.

III. AUTONOMOUS VEHICLE MODELLING

In this section, the lateral dynamical modeling of an autonomous 4-wheeled vehicle with front wheels steering is presented. The simplified bicycle model is used to derive the vehicle model [12]. Since on the curved path, the autonomous vehicle motion is considerably affected by the tire-terrain interaction and banking forces, therefore the effect of these forces is incorporated into the model.

A. LATERAL DYNAMIC MODEL

One of the major challenges for an autonomous vehicle is to keep its lane while moving on the curved path. Unlike the straight path, the effect of lateral forces becomes significant. The 4-wheeled autonomous vehicle motion on a curved path is shown in Fig. 1. The XY-plane represents the reference inertial frame. The center of gravity of the vehicle is denoted by CG, the steering angle is given by δ, while v_x and v_y are the longitudinal and lateral speed, respectively. The yaw angle is denoted by φ.

Assumption 2: Forces on the rear and front wheels of vehicle satisfy $F_i^{\ell} = F_i^{r}$, where $i \in \{f, r\}$ where F_f^{ℓ}, F_f^{r}, F_r^{ℓ} and F_r^{r} are the forces on front-left, front-right, rear-left, and rear-right wheels, respectively.

Remark 1: Following Assumption 2, the combined force on the rear tires F_r and the front tires F_f become twice of the individual wheel forces such that $F_i = 2F_i^{\ell} = 2F_i^{r}$, $i \in \{f, r\}$. Therefore, the autonomous vehicle illustrated in Fig. 1 can be modeled by the rear wheeled drive bicycle model while neglecting the roll and pitch motion.

Assumption 3: We assume that an autonomous vehicle is moving with constant longitudinal speed.

Remark 2: By Assumption 3, the conventional 3-DOF planar model is reduced to the 2-DOF model i.e., lateral position y, and yaw angle φ.

Under Assumption 2 and Assumption 3, the lateral dynamic model of the autonomous vehicle is given by

$$\ddot{y} = \frac{F_{fy} + F_{ry} + F_b}{m} - v_x\dot{\varphi} \tag{8}$$

$$\ddot{\varphi} = \frac{1}{J}\left(d_f F_{fy} - d_r F_{ry}\right) \tag{9}$$

where F_{fy}, F_{ry} are lateral front and rear tire forces, respectively and $F_b = mg\sin(\theta_b)$ is the road banking force where θ_b is the road banking angle. Mass of vehicle and gravitational acceleration is denoted by m and g, respectively. J is the yaw moment of inertia, d_f and d_r are the distances of the front and rear tire from the vehicle's center of gravity.

B. TIRE FORCES

For the autonomous vehicle, the forces acting on tires are of paramount importance. The tire-terrain interaction forces are generally modeled as the nonlinear function of longitudinal slip angle, lateral slip angle, and camber angle, etc. In this article, the Dugoff's tire model is used to determine the lateral tire forces. It is an empirical model, which provides relations for the longitudinal and lateral forces as function of the slip angle and slip ratio. Thus, Dugoff model is a simpler model that accounts for the coupling between the side and longitudinal forces as compared to other linear and nonlinear empirical tire models [44].

The lateral tire forces using this model are given as follows.

$$F_{fy} = \bar{F}_{fy} + \tilde{F}_{fy} \tag{10}$$

$$F_{ry} = \bar{F}_{ry} + \tilde{F}_{ry} \tag{11}$$

where the front and rear nominal forces are represented as $\bar{F}_{fy}$ and $\bar{F}_{ry}$ while forces due to sideslip are denoted by $\tilde{F}_{fy}$ and $\tilde{F}_{ry}$. The front and rear nominal forces are calculated by

$$\bar{F}_{fy} = 2C_f\bar{\alpha}_f \tag{12}$$

$$\bar{F}_{ry} = 2C_r\bar{\alpha}_r \tag{13}$$

where $C_f, \bar{\alpha}_f$ are nominal cornering stiffness and approximate slip angles of the front tire, and C_r and $\bar{\alpha}_r$ are nominal cornering stiffness and approximate slip angles of the rear tire respectively, and can be expressed as:

$$\bar{\alpha}_f = \delta - \frac{\dot{y} + d_f\dot{\varphi}}{v_x} \tag{14}$$

$$\bar{\alpha}_r = -\frac{\dot{y} - d_r\dot{\varphi}}{v_x} \tag{15}$$

Forces due to sideslip are calculated as follows:

$$\tilde{F}_{fy} = \tilde{C}_f \frac{\tan(\alpha_f) f(\lambda_f)}{1+S_x} - \bar{F}_{fy} \tag{16}$$

$$\tilde{F}_{ry} = \tilde{C}_r \frac{\tan(\alpha_r) f(\lambda_r)}{1+S_x} - \bar{F}_{ry} \tag{17}$$

where the S_x is the longitudinal slip ratio. Front and rear tire sideslip angles are given by α_f and α_r while $\tilde{C}_f$ and $\tilde{C}_r$ are cornering stiffness coefficients. The α_f and α_r are given by

$$\alpha_f = \delta - \arctan\left(\frac{\dot{y}+d_f\dot{\varphi}}{v_x}\right) \tag{18}$$

$$\alpha_r = -\arctan\left(\frac{\dot{y}-d_r\dot{\varphi}}{v_x}\right) \tag{19}$$

The function $f(\lambda)$ and $\lambda_i's$ are defined by

$$\lambda_f = \mu_{max} \frac{(1+S_x)F_z}{2\sqrt{\left(\tilde{C}_x S_x\right)^2 + \left(\tilde{C}_y \tan(\alpha_f)\right)^2}} \tag{20}$$

$$\lambda_r = \mu_{max} \frac{(1+S_x)F_z}{2\sqrt{\left(\tilde{C}_x S_x\right)^2 + \left(\tilde{C}_y \tan(\alpha_r)\right)^2}} \tag{21}$$

where $\tilde{C}_y = \tilde{C}_f + \tilde{C}_r$.

$$f(\lambda_i) = \begin{cases} (2-\lambda_i)\lambda_i, & if\ \lambda_i < 1, \\ 1, & if\ \lambda_i \geq 1, \end{cases} \tag{22}$$

The maximum road-tire friction coefficient is denoted by μ_{max}, the coefficients of longitudinal and lateral tire stiffness are $\tilde{C}_x$ and $\tilde{C}_y$ [45].

C. INPUT AFFINE MODEL

By plugging in the expressions for forces in (8) and (9), the resulting input affine autonomous vehicle model is given by

$$\ddot{y} = -\frac{2(C_f+C_r)}{mv_x}\dot{y} - \left[\frac{2(C_f d_f - C_r d_r)}{mv_x} + v_x\right]\dot{\varphi} + \frac{2C_f}{m}\delta + \frac{\tilde{F}_{fy}+\tilde{F}_{ry}+F_b}{m} \tag{23}$$

$$\ddot{\varphi} = -\frac{2\left(C_f d_f^2 + C_r d_r^2\right)}{Jv_x}\dot{\varphi} - \frac{2(C_f d_f - C_r d_r)}{Jv_x}\dot{y} + \frac{2C_f d_f}{J}\delta + \frac{d_f\tilde{F}_{fy} - d_r\tilde{F}_{ry}}{J} \tag{24}$$

We define the yaw and lateral motion in terms of error dynamics as: $\dot{e_1} = \dot{y} + v_x(\varphi - \varphi_d)$ and $e_2 = \varphi - \varphi_d$. The resulting model of the autonomous vehicle in the error dynamics is given by:

$$\ddot{e}_1 = -\frac{2(C_f+C_r)}{mv_x}\dot{e_1} + \frac{2(C_f+C_r)}{m}e_2 - \frac{2(C_f d_f - C_r d_r)}{mv_x}\dot{e_2} + \left[-\frac{2(C_f d_f - C_r d_r)}{mv_x} - v_x\right]\dot{\varphi}_d + \frac{2C_f}{m}\delta + \frac{\tilde{F}_{fy}+\tilde{F}_{ry}+F_b}{m} \tag{25}$$

$$\ddot{e_2} = -\frac{2\left(C_f d_f^2 + C_r d_r^2\right)}{Jv_x}\dot{e_2} - \frac{2(C_f d_f - C_r d_r)}{Jv_x}\dot{e_1} + \frac{2(C_f d_f - C_r d_r)}{J}e_2 + \frac{2C_f d_f}{J}\delta + \frac{d_f\tilde{F}_{fy} - d_r\tilde{F}_{ry}}{J} - \frac{2\left(C_f d_f^2 + C_r d_r^2\right)}{Jv_x}\dot{\varphi}_d - \ddot{\varphi}_d \tag{26}$$

Furthermore, we define $q_1 = e_1; q_2 = \dot{e_1}; q_3 = e_2; q_4 = \dot{e_2}$, then the final system takes the form:

$$\begin{cases} \dot{q}_1 = q_2 \\ \dot{q}_2 = \kappa_1 q_2 + \kappa_2 q_3 + \kappa_3 q_4 + \gamma_1\delta + \omega_1 \end{cases} \tag{27}$$

$$\begin{cases} \dot{q}_3 = q_4 \\ \dot{q}_4 = \kappa_4 q_2 + \kappa_5 q_3 + \kappa_6 q_4 + \gamma_2\delta + \omega_2 \end{cases} \tag{28}$$

where $\kappa_1 = -2(C_f+C_r)/mv_x$, $\kappa_2 = -v_x\kappa_1$, $\kappa_3 = -2(C_f d_f - C_r d_r)/mv_x, \gamma_1 = 2C_f/m, \kappa_4 = -2(C_f d_f - C_r d_r)/Jv_x$, $\kappa_5 = -v_x\kappa_4$, $\kappa_6 = -2\left(C_f d_f^2 + C_r d_r^2\right)/Jv_x, \gamma_2 = 2C_f d_f/J$, $\omega_1 = g\sin(\theta_b) + \frac{\tilde{F}_{fy}+\tilde{F}_{ry}}{m} - (v_x - \kappa_3)\dot{\varphi}_d$, $\omega_2 = \frac{d_f\tilde{F}_{fy} - d_r\tilde{F}_{ry}}{J} + \kappa_6\dot{\varphi}_d - \ddot{\varphi}_d$.

D. MODEL REDUCTION

We define the system parameters using additive uncertainty form as follows:

$$\begin{aligned} \kappa_i &= \bar{\kappa}_i + \Delta_{\kappa_i}; \quad i = 1, 2 \ldots 6 \\ \gamma_m &= \bar{\gamma}_m + \Delta_{\gamma_m}; \quad m = 2, 4 \end{aligned} \tag{29}$$

where nominal parameters are $\bar{\kappa}_i$ and $\bar{\gamma}_m$, the perturbation terms are represented as Δ_{κ_i} and Δ_{γ_m}. Now, the system model with nominal parameters is given by

$$\begin{cases} \dot{q}_1 = q_2 \\ \dot{q}_2 = \bar{\kappa}_1 q_2 + \bar{\kappa}_2 q_3 + \bar{\kappa}_3 q_4 + \bar{\gamma}_1\delta + \Omega_1(q, \delta, \Delta_1, \omega_1) \end{cases} \tag{30}$$

$$\begin{cases} \dot{q}_3 = q_4 \\ \dot{q}_4 = \bar{\kappa}_4 q_2 + \bar{\kappa}_5 q_3 + \bar{\kappa}_6 q_4 + \bar{\gamma}_2\delta + \Omega_2(q, \delta, \Delta_2, \omega_2) \end{cases} \tag{31}$$

Here, the lateral and yaw perturbations are given by Ω_1 and Ω_2, respectively while corresponding overall perturbation in κ_i and γ_m is denoted by Δ_1 and Δ_2.

First, we assume that the control input δ is designed such that the dynamics of (31) are much faster than the dynamics of (30) so within a short period, q_3 reaches its quasi-steady-state $\bar{q}_3$, while q_4 and δ reach to zero. Then the slow dynamics are approximated by

$$\begin{cases} \dot{q}_1 = q_2 \\ \dot{q}_2 = \bar{\kappa}_1 q_2 + \bar{\kappa}_2 \bar{q}_3 + \Omega_2(q, \delta, \Delta_1, \omega_1) \end{cases} \tag{32}$$

where $\bar{q}_3$ is a quasi-steady-state and acts as the auxiliary input for the slow dynamics.

Assumption 4: The perturbation terms Ω_1 and Ω_2 are uniformly bounded as $|\Omega_1| \leq \rho_1$ and $|\Omega_2| \leq \rho_2$.

IV. CONTROLLER DESIGN

In this section control law is devised for a reduced-order system of (31)-(32). Two separate control inputs are designed with (31)-(32) acting as the fast and slow systems, respectively. The fast control input $\boldsymbol{\delta}$ tracks the auxiliary control input $\bar{q}_3$ which eventually result in the stabilization of slow dynamics. In the proceeding text, first conventional SMC is designed for (31)-(32), then SMC with barrier function is designed.

A. CONVENTIONAL SMC DESIGN

To design the conventional SMC, we consider the following sliding surface for slow and fast dynamics, respectively.

$$s_1 = p_1 q_1 + q_2 \tag{33}$$

$$s_2 = p_2 \left(q_3 - \bar{q}_3\right) + q_4 - \dot{\bar{q}}_3 \tag{34}$$

The following Theorem proposes a controller based on the sliding mode control technique.

Theorem 1: For a nonlinear SIMO system (31)-(32) with the sliding manifolds (33)-(34), considering Assumption 4, for control input:

$$\delta = -\frac{1}{\bar{\gamma}_2}\left(-p_2\dot{\bar{q}}_3 - \ddot{\bar{q}}_3 + \bar{\kappa}_4 q_2 + \bar{\kappa}_5 q_3 + q_4\left(p_2 + \bar{\kappa}_6\right) + \mathcal{K}_2 \mathrm{sgn}\left(s_2\right)\right) \tag{35}$$

and with an auxiliary control $\bar{q}_3$:

$$\bar{q}_3 = -\frac{1}{\bar{\kappa}_2}\left(\left(\bar{\kappa}_1 + p_1\right) q_2 + \mathcal{K}_1 \mathrm{sgn}\left(s_1\right)\right) \tag{36}$$

where $\mathcal{K}_i > \rho_i$ for $i = 1, 2$ and $p_2 \gg p_1$, which guarantees the asymptotic stability of the system and the tracking of the desired lateral position and yaw angle is achieved. The initial conditions are defined to be $q_0 = \left(q_{10}, q_{20}, q_{30}, q_{40}\right)$.

Proof: For a Lyapunov function candidate $V_1 = 0.5 s_1^2$ and its derivative $\dot{V}_1 = s_1 \dot{s}_1$, the sliding surface is assumed to be (33)

$$\dot{s}_1 = p_1 q_2 + \bar{\kappa}_1 q_2 + \bar{\kappa}_2 \bar{q}_3 + \Omega_1\left(q, \delta, \Delta_1, \omega_1\right)$$

$$\dot{V}_1 = s_1\left(p_1 q_2 + \bar{\kappa}_1 q_2 + \bar{\kappa}_2 \bar{q}_3 + \Omega_1\left(q, \delta, \Delta_1, \omega_1\right)\right)$$

By employing the auxiliary control input (36)

$$\dot{V}_1 = s_1\left(-\mathcal{K}_1 sgn\left(s_1\right) + \Omega_1\left(q, \delta, \Delta_1, \omega_1\right)\right)$$

Hence, for $\mathcal{K}_1 > \rho_1, \dot{V}_1 \leq 0$, guarantees the asymptotic stability of slow dynamics.

Now to design a controller for slow dynamics, consider the sliding surface (34), with Lyapunov function candidate $V_2 = 0.5 s_2^2$ and $\dot{V}_2 = s_2 \dot{s}_2$ where

$$\dot{s}_2 = p_2(\dot{q}_3 - \dot{\bar{q}}_3) + \dot{q}_4 - \ddot{\bar{q}}_3$$

$$\dot{s}_2 = -p_2\dot{\bar{q}}_3 + \bar{\kappa}_4 q_2 + \bar{\kappa}_5 q_3 + q_4\left(p_2 + \bar{\kappa}_6\right) + \bar{\gamma}_2 \delta + \Omega_2\left(q, \delta, \Delta_2, \omega_2\right) - \ddot{\bar{q}}_3$$

Then

$$\dot{V}_2 = s_2\left(-p_2\dot{\bar{q}}_3 - \ddot{\bar{q}}_3 + \bar{\kappa}_4 q_2 + \bar{\kappa}_5 q_3 + q_4\left(p_2 + \bar{\kappa}_6\right) + \bar{\gamma}_2 \delta + \Omega_2\left(q, \delta, \Delta_2, \omega_2\right)\right)$$

By employing control input (35)

$$\dot{V}_2 = s_2\left(-\mathcal{K}_2 sgn(s_2) + \Omega_2\left(q, \delta, \Delta_2, \omega_2\right)\right)$$

Hence, for $\mathcal{K}_2 > \rho_2, \dot{V}_2 \leq 0$ guarantees the system asymptotic stability.

B. SMC WITH BARRIER FUNCTION

Theorem 2: Under Assumption 1 for the system (31)-(32) and the sliding manifolds (33)-(34), the control input

$$\delta = -\frac{1}{\bar{\gamma}_2}\left(-p_2\dot{\bar{q}}_3 - \ddot{\bar{q}}_3 + \bar{\kappa}_4 q_2 + \frac{q_3}{\mathfrak{h}^2 - q_3^2}|s_2| + \frac{p_2 q_3 \bar{q}_3}{\mathfrak{h}^2 - q_3^2} sign\left(s_2\right) + \bar{\kappa}_5 q_3 + q_4\left(p_2 + \bar{\kappa}_6\right) + \mathcal{K}_2 s_2 + r\left(\frac{q_3}{\sqrt{\left(\mathfrak{h}^2 - q_3^2\right)}} + \sqrt{|2 s_2|}\right) sgn\left(s_2\right)\right) \tag{37}$$

with an auxiliary control $\bar{q}_3$ defined by

$$\bar{q}_3 = -\frac{1}{\bar{\kappa}_2}\left(\left(\bar{\kappa}_1 + p_1\right) q_2 + \frac{q_1}{\hbar^2 - q_1^2}|s_1| + \mathcal{K}_1 s_1 + p\left(\frac{q_1}{\sqrt{\left(\hbar^2 - q_1^2\right)}} + \sqrt{|2 s_1|}\right) \mathrm{sgn}\left(s_1\right)\right) \tag{38}$$

with $\mathcal{K}_i > \rho_i \forall i = 1, 2$, $p, r \in \mathbb{R}$ and $p, r > 0$, then the origin of (31)-(32) is stable. Moreover, the output of the system is guaranteed to track the reference while maintaining the constraints $q_1 < \hbar$ and $q_3 < \mathfrak{h}$.

Proof: We design an auxiliary control $\bar{q}_3$ based on the SMC with barrier function. For sliding surface (33) and Lyapunov function candidate

$$V_1 = |s_1| + \frac{1}{2}\ln\left(\frac{\hbar^2}{\hbar^2 - q_1^2}\right)$$

and the time derivative of V_1 is

$$\dot{V}_1 = \dot{s}_1 \mathrm{sgn}(s_1) + \frac{q_1}{\hbar^2 - q_1^2}\dot{q}_1$$

$$\dot{V}_1 = \mathrm{sgn}(s_1)\left(p_1 q_2 + \bar{\kappa}_1 q_2 + \bar{\kappa}_2 \bar{q}_3 + \Omega_1\left(q, \delta, \Delta_1, \omega_1\right)\right) + \frac{q_1}{\hbar^2 - q_1^2} q_2$$

$$\dot{V}_1 = \mathrm{sgn}\left(s_1\right)\left(p_1 q_2 + \bar{\kappa}_1 q_2 + \bar{\kappa}_2 \bar{q}_3 + \Omega_1\left(q, \delta, \Delta_1, \omega_1\right)\right) + \frac{q_1}{\hbar^2 - q_1^2} s_1 - \frac{p_1 q_1^2}{\hbar^2 - q_1^2}$$

$$\dot{V}_1 = \mathrm{sgn}\left(s_1\right)\left(p_1 q_2 + \bar{\kappa}_1 q_2 + \bar{\kappa}_2 \bar{q}_3 + \frac{q_1}{\hbar^2 - q_1^2}|s_1| + \Omega_1\left(q, \delta, \Delta_1, \omega_1\right)\right)$$

By employing auxiliary control input (38)

$$\dot{V}_1 = -\mathcal{K}_1 |s_1| - p\left(\frac{q_1}{\sqrt{\hbar^2 - q_1^2}} + \sqrt{|2s_1|}\right) + \Omega_1 (q, \delta, \Delta_1, \omega_1) (sgn (s_1))$$

$$\dot{V}_1 \leq -p\left(\frac{q_1}{\sqrt{\hbar^2 - q_1^2}} + \sqrt{|2s_1|}\right)$$

$$\dot{V}_1 \leq -p\left(\sqrt{\frac{q_1^2}{\hbar^2 - q_1^2}} + \sqrt{|2s_1|}\right)$$

by using Lemma 2

$$\dot{V}_1 \leq -p\left(\sqrt{\ln\left(\frac{\hbar^2}{\hbar^2 - q_1^2}\right)} + \sqrt{|2s_1|}\right)$$

$$\dot{V}_1 \leq -p\sqrt{\ln\left(\frac{\hbar^2}{\hbar^2 - q_1^2}\right) + |2s_1|}$$

$$\dot{V}_1 \leq -p\sqrt{2V_1}$$

Now to design a controller for slow dynamics, consider the sliding surface (34), with Lyapunov function candidate

$$V_2 = |s_2| + \frac{1}{2}\ln\left(\frac{\mathfrak{h}^2}{\mathfrak{h}^2 - q_3^2}\right)$$

and the time derivative of V_1 is

$$\dot{V}_2 = \dot{s_2} sgn(s_2) + \frac{q_3}{\mathfrak{h}^2 - q_3^2}\dot{q}_3$$

$$\dot{s_2} = p_2 q_4 - p_2\dot{\bar{q}}_3 + \bar{\kappa}_4 q_2 + \bar{\kappa}_5 q_3 + \bar{\kappa}_6 q_4 + \bar{\gamma}_2\delta + \Omega_2 (q, \delta, \Delta_2, \omega_2) - \ddot{\bar{q}}_3$$

$$\dot{s}_2 = -p_2\dot{\bar{q}}_3 + \bar{\kappa}_4 q_2 + \bar{\kappa}_5 q_3 + q_4 (p_2 + \bar{\kappa}_6) + \bar{\gamma}_2\delta + \Omega_2 (q, \delta, \Delta_2, \omega_2) - \ddot{\bar{q}}_3$$

$$\dot{V}_2 = \text{sgn}\,(s_2)\left(-p_2\dot{\bar{q}}_3 - \ddot{\bar{q}}_3 + \bar{\kappa}_4 q_2 + \bar{\kappa}_5 q_3 + q_4 (p_2 + \bar{\kappa}_6) + \bar{\gamma}_2\delta + \Omega_2 (q, \delta, \Delta_2, \omega_2)\right) + \frac{q_3}{\mathfrak{h}^2 - q_3^2} q_4$$

$$\dot{V}_2 = \text{sgn}\,(s_2)\left(-p_2\dot{\bar{q}}_3 - \ddot{\bar{q}}_3 + \bar{\kappa}_4 q_2 + \bar{\kappa}_5 q_3 + q_4 (p_2 + \bar{\kappa}_6) + \bar{\gamma}_2\delta + \Omega_2 (q, \delta, \Delta_2, \omega_2)\right) + \frac{q_3}{\mathfrak{h}^2 - q_3^2}\left(s_2 + p_2\bar{q}_3\right) - \frac{p_2 q_3^2}{\mathfrak{h}^2 - q_3^2}$$

$$\dot{V}_2 = \text{sgn}\,(s_2)\left(-p_2\dot{\bar{q}}_3 - \ddot{\bar{q}}_3 + \bar{\kappa}_4 q_2 + \frac{q_3}{\mathfrak{h}^2 - q_3^2}|s_2| + \frac{p_2 q_3 \bar{q}_3}{\mathfrak{h}^2 - q_3^2}\text{sgn}\,(s_2) + \bar{\kappa}_5 q_3 + q_4 (p_2 + \bar{\kappa}_6) + \bar{\gamma}_2\delta + \Omega_2 (q, \delta, \Delta_2, \omega_2)\right)$$

By employing control input (37)

$$\dot{V}_2 = \text{sgn}\,(s_2)\left(-\mathcal{K}_2 s_2 - r\left(\frac{q_3}{\sqrt{(\mathfrak{h}^2 - q_3^2)}} + \sqrt{|2s_2|}\right) \times \text{sgn}(s_2) + \Omega_2 (q, \delta, \Delta_2, \omega_2)\right)$$

$$\dot{V}_2 = \left(-\mathcal{K}_2 |s_2| - r\left(\frac{q_3}{\sqrt{(\mathfrak{h}^2 - q_3^2)}} + \sqrt{|2s_2|}\right)\right) + \Omega_2 (q, \delta, \Delta_2, \omega_2) (\text{sgn}\,(s_2))$$

$$\dot{V}_2 = -\mathcal{K}_2 |s_2| - r\left(\frac{q_3}{\sqrt{(\mathfrak{h}^2 - q_3^2)}} + \sqrt{|2s_2|}\right) + \Omega_2 (q, \delta, \Delta_2, \omega_2) (\text{sgn}\,(s_2))$$

$$\dot{V}_2 \leq -r\left(\frac{q_3}{\sqrt{(\mathfrak{h}^2 - q_3^2)}} + \sqrt{|2s_2|}\right)$$

$$\dot{V}_2 \leq -r\left(\sqrt{\frac{q_3^2}{\mathfrak{h}^2 - q_3^2}} + \sqrt{|2s_2|}\right)$$

by using Lemma 2

$$\dot{V}_2 \leq -r\left(\sqrt{\ln\left(\frac{\mathfrak{h}^2}{\mathfrak{h}^2 - q_3^2}\right)} + \sqrt{|2s_2|}\right)$$

$$\dot{V}_2 \leq -r\sqrt{\ln\left(\frac{\mathfrak{h}^2}{\mathfrak{h}^2 - q_3^2}\right) + |2s_2|}$$

$$\dot{V}_2 \leq -r\sqrt{2V_2}$$

Corollary 1: Theorem 2 not only guarantees the output trajectory tracking but also enables to stabilize the slow and fast dynamics in the finite time. Moreover, if the initial conditions are defined to be $q_0 = (q_{10}, q_{20}, q_{30}, q_{40})$ and with $\hbar_a = \sqrt{2}\,p$, then the upper bound on the settling time function $T_{slow} : \mathbb{R}^2 \to \mathbb{R}^+$ is given as:

$$T_{slow} \leq \frac{1}{p_1}\ln\left(\frac{\hbar}{0.02}\right) + \frac{2}{\hbar_a}\sqrt{|p_1 q_{10} + q_{20}| + \frac{1}{2}\ln\left(\frac{\hbar^2}{\hbar^2 - q_{10}^2}\right)} \tag{39}$$

while the convergence of fast states is guaranteed in

$$T_{fast} \leq \frac{1}{p_2}\ln\left(\frac{\mathfrak{h}}{0.02}\right) + \frac{2}{\mathrm{k}_b}\sqrt{|p_2 q_{30} + q_{40}| + \frac{1}{2}\ln\left(\frac{\mathfrak{h}^2}{\mathfrak{h}^2 - q_{30}^2}\right)} \tag{40}$$

where $\hbar_b = \sqrt{2}r$.

Proof: With $\dot{V} = -\hbar_b\sqrt{V}$ and $\hbar_b = \sqrt{2}\,r$

$$\frac{dV}{\sqrt{V}} = -\hbar_b dt$$

By using the fact that $V = 0; \forall t \geq T$, the solution of the above equation and is given by;

$$T_r \leq \frac{2}{\hbar_b}\sqrt{V_0}$$

where V_0 is the initial value of the Lyapunov function and is given by;

$$V_0 = \left|p_2\left(q_{30} + \bar{q}_{30}\right) + q_{40}\right| + \frac{1}{2}\ln\left(\frac{\mathfrak{h}^2}{\mathfrak{h}^2 - q_{30}^2}\right)$$

Since $\bar{q}_3$ is an auxiliary input that is zero initially and $q_{30} = q_3(0), q_{40} = q_4(0), \bar{q}_{30} = \bar{q}_3(0) = 0$.

$$V_0 = \left|p_1 q_{10} + q_{20}\right| + \frac{1}{2}\ln\left(\frac{\hbar^2}{\hbar^2 - q_{10}^2}\right)$$

where $q_{10} = q_1(0), q_{20} = q_2(0)$. The time T_r is the time taken by the states to reach the sliding surface. Now we will evaluate the time T_s for states to stabilize to the equilibrium point after reaching the sliding surface. The sliding surface is given by $s_1 = p_1 q_1 + q_2 = 0$ where

$$\dot{q_1} = -p_1 q_1$$

The solution of the above equation is $q_1 = q_{10}^* e^{-p_1 t}$. Therefore, for the decaying signal after 4τ, only 2% of q_{10}^* will be available. The time required for q_1 to reach its equilibrium point (98% settling time criteria) is calculated by

$$\begin{aligned}\frac{0.02}{q_{10}^*} &= e^{-p_1 t}\\ q_{10}^* &= \hbar\\ t &= -\frac{1}{p_1}\ln\left(\frac{0.02}{\hbar}\right)\\ T_s &\leq \frac{1}{p_1}\ln\left(\frac{\hbar}{0.02}\right)\end{aligned}$$

Hence, the total settling time for the slow states to converge to the origin is

$$T_{slow} = T_s + T_r$$

$$T_{slow} \leq \frac{1}{p_1}\ln\left(\frac{\hbar}{0.02}\right) + \frac{2}{\hbar_a}\sqrt{\left|p_1 q_{10} + q_{20}\right| + \frac{1}{2}\ln\left(\frac{\hbar^2}{\hbar^2 - q_{10}^2}\right)}$$

Following a similar methodology, the convergence of fast states is guaranteed in

$$T_{fast} \leq \frac{1}{p_2}\ln\left(\frac{\mathfrak{h}}{0.02}\right) + \frac{2}{\hbar_b}\sqrt{\left|p_2 q_{30} + q_{40}\right| + \frac{1}{2}\ln\left(\frac{\mathfrak{h}^2}{\mathfrak{h}^2 - q_{30}^2}\right)}$$

Remark 3: The T_{slow} and T_{fast} facilitate the selection of controller gains that result in the finite-time stability of slow and fast dynamics such that $T_{fast} \ll T_{slow}$ and hence model reduction is validated.

TABLE 1. Autonomous vehicle parameters [46].

Symbol	Description	Value
m	Mass of Vehicle	1500kg
g	Gravitational acceleration	$9.81 m/s^2$
J	Yaw inertia	$1350\ kgm^2$
d_f	Front wheels distance from CG	$1.5m$
d_r	Rear wheels distance from CG	$2m$
C_x	Longitudinal tire stiffness	$70\ kN/rad$
C_f	Front Tire Concerning Stiffness	$55\ kN/rad$
C_r	Rear Tire Concerning Stiffness	$120\ kN/rad$

V. SIMULATION RESULTS

This section presents the numerical simulation results of the controller designed for lateral control of the autonomous vehicle. The conventional SMC and SMC with barrier function are compared to examine the performance of the proposed technique. The results are obtained for tracking a realistic smooth trajectory given as $\varphi_d = \left[-\text{sech}^2(2t-17) + \text{sech}^2(2t-42)\right]$ and $y_d = 0.5 v_x\left[tanh(2t-17) - tanh(2t-42)\right]$.

The parameters for the autonomous vehicle are given in Table-1. The vehicle is assumed to be moving with a constant longitudinal speed $v_x = 20 ms^{-1}$ while initial conditions for the lateral position, lateral speed, yaw angle, and yaw rate are set to $0m$, $0ms^1$, $0\ rad$ and $0\ rad/s$, respectively. The slip ratio S_x is assumed to be between 0.1 to 0.4. The road banking angle, which is an unknown switching disturbance, is presumed to be $0.087 rad$. The lateral tire forces are modelled using the Dugoff tire model. It is observed that the upper bound on Ω_1 and Ω_2 were $\rho_1 = 0.6$ and $\rho_2 = 6.7$, respectively. The vehicle parameters are perturbed 12% of their nominal values. The simulations are performed for a fixed step size of $2ms$.

The absolute bound on the lateral position $\hbar_c$ is defined by $\hbar_c = 20.75m$ while yaw angle is bounded by $\mathfrak{h}_c = 1.0524 rad$. Since maximum absolute values of y_d and φ_d are $20m$ and $1rad$, therefore by Assumption 2, the $\hbar_b = \hbar_c - \max(y_d) = 0.75m$ and $\mathfrak{h}_b = \mathfrak{h}_c - \max(\varphi_d) = 0.0524 rad = 3°$. The settling time functions (39) and (40) are taken into consideration to evaluate the controller gains. By setting $T_{fast} = 1.10s$ and $T_{slow} = 7.86s$, we obtained the controller gains $p_1 = 0.5, p_2 = 3, \mathcal{K}_1 = 0.5, \mathcal{K}_2 = 2, p = 1, r = 1$. For simulations of both conventional SMC and SMC with barrier function, the same controller gains are utilized. It is stressed that T_{fast} and T_{slow} only help in choosing gains. The cumulative controller may settle in different time and hence we cannot observe these times in simulation results.

The comparison graphs of the lateral position of the autonomous vehicle for tracking y_d is given in Figure 2. Both conventional SMC and SMC with barrier function track the reference It can be observed that the tracking performance of conventional SMC deteriorates when the reference lateral trajectory changes. The comparison of lateral position error is given in Figure 3. It is evident that the conventional SMC defies the desired error bound $\hbar_c$. On the other hand, SMC

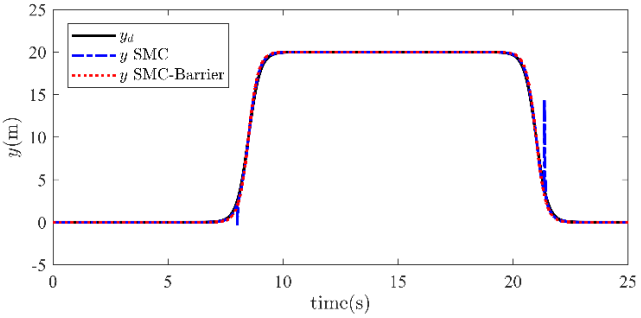

FIGURE 2. Lateral position tracking using SMC and SMC with barrier function.

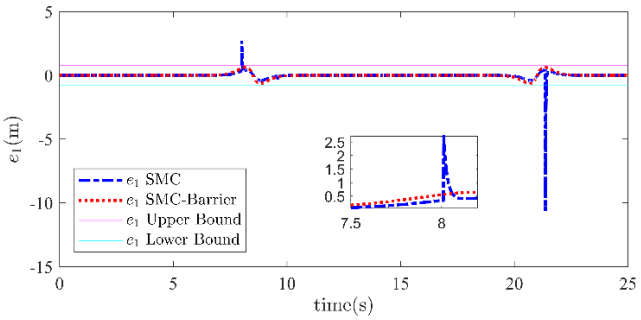

FIGURE 3. Lateral position tracking error using SMC and SMC with barrier function.

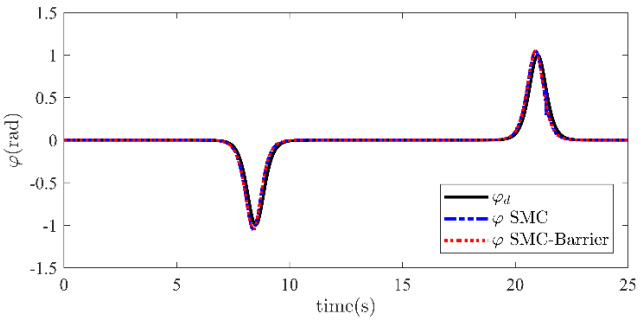

FIGURE 4. Yaw angle tracking using SMC and SMC with barrier function.

with barrier function ensures that lateral position remains in desired bound during trajectory tracking. Furthermore, it is evident from Figure. 2,3, that SMC with barrier function exhibits better lateral position tracking as compared to conventional SMC.

In Figure 4, the yaw angle tracking of the autonomous vehicle for conventional SMC and SMC with barrier function is shown. Both controllers exhibit their robustness against disturbances and parametric uncertainties while tracking the desired yaw reference. Moreover, the results of Figure 5 depict that SMC with barrier function outperforms the conventional SMC. The conventional SMC not only displays relatively higher error but also violates the yaw error constraint $\mathfrak{h}_c$. Conversely, SMC with barrier function satisfies the desired output constraints and hence demonstrates improved performance as compared to conventional SMC.

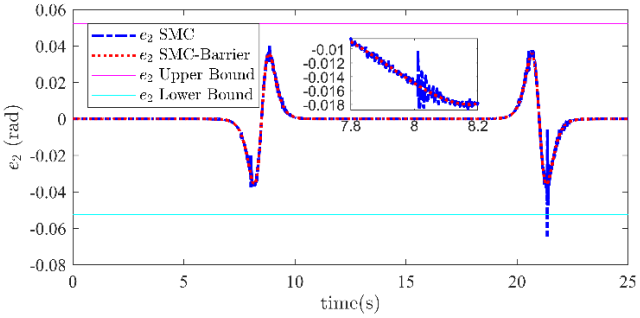

FIGURE 5. Yaw angle tracking error using SMC and SMC with barrier function.

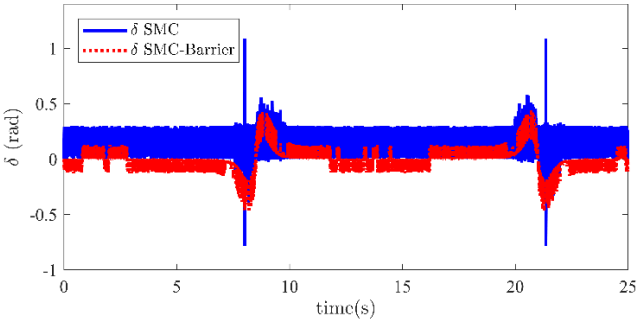

FIGURE 6. Control input for SMC and SMC with barrier function.

The control input for both controllers is compared in Figure 6. From the results, it can be deduced that SMC with barrier function results in less chattering as compared to conventional SMC. Since, in both controllers the resulting control effort is proportional to the magnitude of the disturbances; therefore, the centre of magnitude of the control effort is non-zero.

VI. CONCLUSION

In this paper, a robust control technique is proposed for the autonomous vehicle lateral dynamics in the presence of lateral tire forces, road curvature, and parametric uncertainties. The autonomous vehicle model is reduced to slow and fast dynamics and SMC with barrier function is employed to track the system's desired outputs while restricting the output in certain bounds. From the numerical simulations, it is evident that SMC with barrier function achieved better tracking performance as compared to conventional SMC.

REFERENCES

[1] C. Badue, R. Guidolini, R. V. Carneiro, P. Azevedo, V. B. Cardoso, A. Forechi, L. Jesus, R. Berriel, T. M. Paixao, F. Mutz, and L. D. P. Veronese, "Self-driving cars: A survey," *Expert Syst. Appl.*, vol. 165, Mar. 2020, Art. no. 113816.

[2] M. H. Hebert, C. E. Thorpe, and A. Stentz, *Intelligent Unmanned Ground Vehicles: Autonomous Navigation Research at Carnegie Mellon*. New York, NY, USA: Springer, 2012.

[3] J. Li, H. Bao, X. Han, F. Pan, W. Pan, F. Zhang, and D. Wang, "Real-time self-driving car navigation and obstacle avoidance using mobile 3D laser scanner and GNSS," *Multimedia Tools Appl.*, vol. 76, no. 21, pp. 23017–23039, Nov. 2017.

[4] B. Paden, M. Cap, S. Z. Yong, D. Yershov, and E. Frazzoli, "A survey of motion planning and control techniques for self-driving urban vehicles," *IEEE Trans. Intell. Vehicles*, vol. 1, no. 1, pp. 33–55, Mar. 2016.

[5] Q. Luo, Y. Cao, J. Liu, and A. Benslimane, "Localization and navigation in autonomous driving: Threats and countermeasures," *IEEE Wireless Commun.*, vol. 26, no. 4, pp. 38–45, Aug. 2019.

[6] R. Wang, H. Jing, C. Hu, F. Yan, and N. Chen, "Robust H_∞ path following control for autonomous ground vehicles with delay and data dropout," *IEEE Trans. Intell. Transp. Syst.*, vol. 17, no. 7, pp. 2042–2050, Jul. 2016.

[7] N. H. Amer, H. Zamzuri, K. Hudha, and Z. A. Kadir, "Modelling and control strategies in path tracking control for autonomous ground vehicles: A review of state of the art and challenges," *J. Intell. Robot. Syst.*, vol. 86, no. 2, pp. 225–254, May 2017.

[8] C. M. Filho, D. F. Wolf, V. Grassi, and F. S. Osorio, "Longitudinal and lateral control for autonomous ground vehicles," in *Proc. IEEE Intell. Vehicles Symp.*, Jun. 2014, pp. 588–593.

[9] J. Guanetti, Y. Kim, and F. Borrelli, "Control of connected and automated vehicles: State of the art and future challenges," *Annu. Rev. Control*, vol. 45, pp. 18–40, Jan. 2018.

[10] J. Huang, "Vehicle longitudinal control," in *Handbook of Intelligent Vehicles*. London, U.K.: Springer, 2012, pp. 167–190.

[11] B. Arifin, B. Y. Suprapto, S. A. D. Prasetyowati, and Z. Nawawi, "The lateral control of autonomous vehicles: A review," in *Proc. Int. Conf. Electr. Eng. Comput. Sci. (ICECOS)*, Oct. 2019, pp. 277–282.

[12] R. Rajamani, *Vehicle Dynamics and Control*. New York, NY, USA: Springer, 2011.

[13] Q. Liu, Y. Liu, C. Liu, B. Chen, W. Zhang, L. Li, and X. Ji, "Hierarchical lateral control scheme for autonomous vehicle with uneven time delays induced by vision sensors," *Sensors*, vol. 18, no. 8, p. 2544, Aug. 2018.

[14] R. Marino, S. Scalzi, and M. Netto, "Nested PID steering control for lane keeping in autonomous vehicles," *Control Eng. Pract.*, vol. 19, no. 12, pp. 1459–1467, Dec. 2011.

[15] D.-C. Liaw and W.-C. Chung, "A feedback linearization design for the control of vehicle's lateral dynamics," *Nonlinear Dyn.*, vol. 52, no. 4, pp. 313–329, 2008.

[16] C. M. Kang, W. Kim, and C. C. Chung, "Observer-based backstepping control method using reduced lateral dynamics for autonomous lane-keeping system," *ISA Trans.*, vol. 83, pp. 214–226, Dec. 2018.

[17] P. Wang, S. Gao, L. Li, S. Cheng, and L. Zhao, "Automatic steering control strategy for unmanned vehicles based on robust backstepping sliding mode control theory," *IEEE Access*, vol. 7, pp. 64984–64992, 2019.

[18] W. Zhang, "A robust lateral tracking control strategy for autonomous driving vehicles," *Mech. Syst. Signal Process.*, vol. 150, Mar. 2021, Art. no. 107238.

[19] A. Norouzi, M. Masoumi, A. Barari, and S. Farrokhpour Sani, "Lateral control of an autonomous vehicle using integrated backstepping and sliding mode controller," *Proc. Inst. Mech. Eng., K, J. Multi-Body Dyn.*, vol. 233, no. 1, pp. 141–151, Mar. 2019.

[20] G. Tagne, R. Talj, and A. Charara, "Higher-order sliding mode control for lateral dynamics of autonomous vehicles, with experimental validation," in *Proc. IEEE Intell. Vehicles Symp. (IV)*, Jun. 2013, pp. 678–683.

[21] X. Wang, M. Fu, H. Ma, and Y. Yang, "Lateral control of autonomous vehicles based on fuzzy logic," *Control Eng. Pract.*, vol. 34, pp. 1–17, Jan. 2015.

[22] C. Hu, Y. Chen, and J. Wang, "Fuzzy observer-based transitional path-tracking control for autonomous vehicles," *IEEE Trans. Intell. Transp. Syst.*, early access, Mar. 16, 2020, doi: 10.1109/TITS.2020.2979431.

[23] W. Chen, R. Zhang, L. Zhao, H. Wang, and Z. Wei, "Control of chaos in vehicle lateral motion using the sliding mode variable structure control," *Proc. Inst. Mech. Eng., D, J. Automobile Eng.*, vol. 233, no. 4, pp. 776–789, Mar. 2019.

[24] K. Akermi, S. Chouraqui, and B. Boudaa, "Novel SMC control design for path following of autonomous vehicles with uncertainties and mismatched disturbances," *Int. J. Dyn. Control*, vol. 8, no. 1, pp. 254–268, Mar. 2020.

[25] K. Xu, X. Wu, M. Ma, and Y. Zhang, "Energy-based output feedback control of the underactuated 2DTORA system with saturated inputs," *Trans. Inst. Meas. Control*, vol. 42, no. 14, pp. 2822–2829, Oct. 2020.

[26] H. T. Nguyen, M. T. Nguyen, T. T. Doan, and C. P. Vo, "Designing PID-fuzzy controller for pendubot system," *Robotica Manage.*, vol. 22, no. 2, pp. 21–27, 2017.

[27] D. Li, D. Zhao, Q. Zhang, and Y. Chen, "Reinforcement learning and deep learning based lateral control for autonomous driving [application notes]," *IEEE Comput. Intell. Mag.*, vol. 14, no. 2, pp. 83–98, May 2019.

[28] D. H. Vu, S. Huang, and T. D. Tran, "Hierarchical robust fuzzy sliding mode control for a class of simo under-actuated systems with mismatched uncertainties," *Telkomnika*, vol. 17, no. 6, pp. 3027–3043, 2019.

[29] D. Qian, J. Yi, and D. Zhao, "Hierarchical sliding mode control for a class of SIMO under-actuated systems," *Control Cybern.*, vol. 37, no. 1, p. 159, 2008.

[30] J. Jiang and A. Astolfi, "Lateral control of an autonomous vehicle," *IEEE Trans. Intell. Vehicles*, vol. 3, no. 2, pp. 228–237, Jun. 2018.

[31] S. A. A. Shah, B. Gao, N. Ahmed, C. Liu, and A. Rauf, "Disturbance observer-based sliding mode control of TORA system for floating wind turbines," presented at the IEEE 9th Annu. Int. Conf. CYBER Technol. Automat., Control, Intell. Syst. (CYBER), 2019, doi: 10.1109/CYBER46603.2019.9066505.

[32] J. Lee, R. Mukherjee, and H. K. Khalil, "Output feedback stabilization of inverted pendulum on a cart in the presence of uncertainties," *Automatica*, vol. 54, pp. 146–157, Apr. 2015.

[33] A. Chakrabortty and M. Arcak, "Time-scale separation redesigns for stabilization and performance recovery of uncertain nonlinear systems," *Automatica*, vol. 45, no. 1, pp. 34–44, Jan. 2009.

[34] A. Raza, F. M. Malik, N. Mazhar, H. Ullah, and R. Khan, "Finite-time trajectory tracking control of output-constrained uncertain quadrotor," *IEEE Access*, vol. 8, pp. 215603–215612, 2020.

[35] N. Ahmadian, A. Khosravi, and P. Sarhadi, "Managing driving disturbances in lateral vehicle dynamics via adaptive integrated chassis control," *Proc. Inst. Mech. Eng., K, J. Multi-Body Dyn.*, vol. 235, no. 1, pp. 122–133, Mar. 2021.

[36] W. Qin, "Unit sliding mode control for disturbed crowd dynamics system based on integral barrier Lyapunov function," *IEEE Access*, vol. 8, pp. 91257–91264, 2020.

[37] S. I. Han, J. Y. Cheong, and J. M. Lee, "Barrier Lyapunov function-based sliding mode control for guaranteed tracking performance of robot manipulator," *Math. Problems Eng.*, vol. 2013, Nov. 2013, Art. no. 978241.

[38] B. Zhu, X. Wang, and K.-Y. Cai, "Approximate trajectory tracking of input-disturbed PVTOL aircraft with delayed attitude measurements," *Int. J. Robust Nonlinear Control*, vol. 20, no. 14, pp. 1610–1621, Sep. 2010.

[39] M. Innocenti, L. Greco, and L. Pollini, "Sliding mode control for two-time scale systems: Stability issues," *Automatica*, vol. 39, no. 2, pp. 273–280, Feb. 2003.

[40] H. K. Khalil, *High-Gain Observers in Nonlinear Feedback Control*. Philadelphia, PA, USA: SIAM, 2017.

[41] K. P. Tee, S. S. Ge, and E. H. Tay, "Barrier Lyapunov functions for the control of output-constrained nonlinear systems," *Automatica*, vol. 45, no. 4, pp. 918–927, Apr. 2009.

[42] B. Ren, S. S. Ge, K. P. Tee, and T. H. Lee, "Adaptive neural control for output feedback nonlinear systems using a barrier Lyapunov function," *IEEE Trans. Neural Netw.*, vol. 21, no. 8, pp. 1339–1345, Aug. 2010.

[43] Y. Sun, B. Chen, C. Lin, and H. Wang, "Finite-time adaptive control for a class of nonlinear systems with nonstrict feedback structure," *IEEE Trans. Cybern.*, vol. 48, no. 10, pp. 2774–2782, Oct. 2018.

[44] Z. Shiller and S. Sundar, "Optimal emergency maneuvers of automated vehicles," Univ. California, Los Angeles, CA, USA, Tech. Rep. UCB-ITS-PRR-96-32, 1996.

[45] L.-H. Zhao, Z.-Y. Liu, and H. Chen, "Design of a nonlinear observer for vehicle velocity estimation and experiments," *IEEE Trans. Control Syst. Technol.*, vol. 19, no. 3, pp. 664–672, May 2011.

[46] A. M. Ribeiro, A. R. Fioravanti, A. Moutinho, and E. C. D. Paiva, "Nonlinear state-feedback design for vehicle lateral control using sum-of-squares programming," *Vehicle Syst. Dyn.*, pp. 1–27, Nov. 2020. [Online]. Available: https://www.tandfonline.com/doi/abs/10.1080/00423114.2020.1844905?journalCode=nvsd20&

RAMEEZ KHAN received the B.S. degree in electronics engineering from COMSATS University Islamabad, Abbottabad, Pakistan, in 2012, and the M.S. degree in electrical engineering from the National University of Science and Technology, Islamabad, Pakistan, in 2014, where he is currently pursuing the Ph.D. degree. His research interests include the development of nonlinear observers, control of underactuated systems, autonomous vehicles, and robotic control systems.

FAHAD MUMTAZ MALIK received the B.Sc., M.S., and Ph.D. degrees from the National University of Sciences and Technology, Islamabad, Pakistan, in 2004, 2006, and 2009, respectively. He is an Associate Professor with the Department of Electrical Engineering, College of Electrical and Mechanical Engineering, National University of Sciences and Technology. He is the author of over 60 papers in peer-reviewed international journals and conferences. His research interests include the control of service and field robots, machine learning, artificial intelligence, and nonlinear control systems.

NAVEED MAZHAR received the B.S. degree in electrical (electronics) engineering from COMSATS University Islamabad, Abbottabad, Pakistan, in 2013, and the M.S. degree in electrical engineering from the National University of Science and Technology, Islamabad, Pakistan, in 2016, where he is currently pursuing the Ph.D. degree. His research interests include multi-agent systems, modeling, networked control systems, fixed-time control, and linear and nonlinear control design for dynamic systems.

ABID RAZA received the B.S. degree in electronics engineering from COMSATS University Islamabad, Abbottabad, Pakistan, in 2012, and the M.S. degree in electrical engineering from the National University of Science and Technology, Islamabad, Pakistan, in 2014, where he is currently pursuing the Ph.D. degree. His research interests include nonlinear control, high gain observers, flight control systems, robust control of UAVs, and robotics.

RAJA AMER AZIM received the B.E. degree in mechanical engineering from the University of Engineering and Technology, Taxila, Pakistan, in 1993, the M.S. degree in mechanical engineering from the University of New South Wales, Australia, in 2001, and the Ph.D. degree in mechanical engineering, in 2015. He joined the Faculty of Department of Mechanical Engineering with the College of EME, National University of Sciences and Technology, Islamabad, Pakistan. With over two decades of experience in mechanical product development in research and development and academic organizations. He is currently serving as an Assistant Professor with the Department of Mechanical Engineering, College of EME, National University of Sciences and Technology. He has various reputed journal and conference publications to his name. He is working on several funded research projects. His research interests include vehicle dynamics and control systems, mechanical system design, and autonomous vehicle systems.

HAMEED ULLAH received the B.Sc. degree in electrical engineering from UET, Peshawar, Pakistan, in 2015, and the M.S. degree in electrical engineering from the National University of Sciences and Technology, Islamabad, Pakistan, in 2019. His research interests include the flexible link robotic manipulators, robust state estimation, high gain observer, linear and nonlinear control systems, robotics, modeling, UAVs, sliding mode control, and robust control for underactuated mechanical systems.